STUDIA UBB CHEMIA, LVIII, 4, 2013 (p. 227-241)
(RECOMMENDED CITATION)

Dedicated to Professor Liviu Literat
On the occasion of his 85th birthday

AN ANALYSIS OF THE STABILIZATION MECHANISM OF REVERSE FLOW REACTORS WITH APPLICATION IN CATALYTIC VOC COMBUSTION

IOANA STOICA[a], IONUȚ BANU[a,*], GRIGORE BOZGA[a]

ABSTRACT. The aim of the work is a thorough theoretical analysis regarding the time evolutions of state variables during the stabilization of temperature and composition profiles, for a fixed catalytic bed reactor, operated in forced unsteady state regime by periodically changing the flow direction. The decontamination of lean waste gases by VOC combustion over a commercial Pt/alumina catalyst with non-uniform distribution of Pt is considered as a case study. The process is mathematically described by a heterogeneous one-dimensional model. The simulation results evidence that the stabilized (pseudo-steady) state regime is achieved when the amount of heat generated during a cycle equals the amount of heat withdrawn from the bed by gaseous mixture.

Keywords: *packed bed, reverse flow, unsteady-state, process simulation, sensitivity analysis*

INTRODUCTION

The reverse flow reactor (RFR) is a gas-solid catalytic packed or monolith bed reactor operated in forced unsteady-state regime by periodical change of feed flow direction. The main advantage in this technique consists in the possibility to realize the autothermal operation, even at low volatile organic compounds (VOC) concentrations, by achieving appropriate temperature profiles along the bed. One of the important applications suitable for this apparatus is the VOC elimination from lean gaseous mixtures by catalytic combustion [1-5].

[a] *University Politehnica of Bucharest, Faculty of Applied Chemistry and Material Science, Department of Chemical and Biochemical Engineering, Bucharest, Romania.*
* *Corresponding author: Ionut Banu, University Politehnica of Bucharest, Faculty of Applied Chemistry and Material Science, Department of Chemical and Biochemical Engineering, 313-Spl. Independentei, sect. 6, 060042 Bucharest, Romania, Tel: +021 4023938, Email: i_banu@chim.upb.ro*

Kolios [6] referred to the RFR as a multi-functional apparatus, as it is embodying in a single device the functions of reactor and heat exchanger.

Generally, the mechanisms of unsteady processes are more complex, as compared with processes occurring at steady state. In the development of their mathematical models, particular unsteady state correlations should be used for calculation of the kinetics of chemical and physical process steps. However, in the absence of such data, analysis and design calculations for unsteady processes are usually based on correlations based on steady state data.

This paper aims to highlight the features of auto-thermal operated reverse flow packed bed reactors, in VOCs catalytic combustion applications. There are emphasized the interplay of the physical and chemical process steps, as well as the conditions that ensure the time stabilization (achievement of pseudo-steady state).

The principle of RFR operation consists in feeding the gaseous reactants mixture, usually at room temperature, over the hot catalytic bed, the gas pre-heating to the reaction temperature being assured by the entry zone of the packed bed, which is progressively cooled. Thus, it appears a cooled zone of the bed, which is slowly moving in the direction of the gas flow. If the direction of gas flow in the reactor is reversed with an adequate frequency, after a sufficient number of reversals, a succession of axial temperature profiles, insuring the consumption of reactant, are achieved and stabilized inside the bed. A sketch of the reactor connections needed for reactants supply and products removal for reverse flow operation are shown in Figure 1. The reaction mixture can be fed either from the left to the right (when the valves 1 and 4 are open, and 2 and 3 closed) or from the right to the left (2 and 3 are open, 1 and 4 are closed). In the case of irreversible reactions, the extreme zones of reactor bed (I and III in Figure 1) have roles only in heat accumulation and its transfer to the gas phase, the chemical reaction taking place in the central zone (II). Consequently, in the zones I and III it can be used an inert solid (non-catalytic material), preferentially having a high specific heat capacity. This is also the bed structure considered in the present study [1, 2].

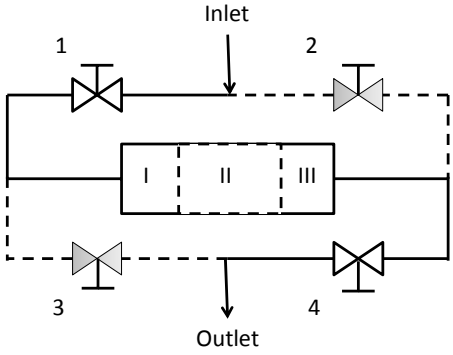

Figure 1. Connection scheme of a reverse flow operated packed bed reactor

MATHEMATICAL MODEL AND NUMERICAL METHOD

The present theoretical analysis is based on process description by a heterogeneous, one-dimensional axial dispersion model, considering, in addition to convective transport in the gas phase, a mechanism of mass and heat dispersion in axial direction. The model neglects the contribution of the metallic wall in the axial heat transport (the heat transferred from the packed bed to the wall, and then through the wall in the axial direction is not taken into account). In addition, the thermal regime is adiabatic, the gas phase behavior is ideal, the pressure drop in the packed bed is neglected and the chemical reactions are considered only on the surface of the catalyst.

The mass and heat balances in the gaseous and solid phases of the bed are expressed by equations (1) to (4). They apply for both catalyst and inert zones of the packed bed, for the latter canceling the terms which represent the contributions of the chemical reaction ($r_A = 0$).

$$\varepsilon \frac{\partial Y_{AG}}{\partial t} = \varepsilon D_L \frac{\partial^2 Y_{AG}}{\partial z^2} - u \frac{\partial Y_{AG}}{\partial z} - k_G a_v C_t \left(Y_{AG} - Y_{AS} \right) \tag{1}$$

$$k_G a_v C_t \left(Y_{AG} - Y_{AS} \right) = \rho_{cat} \eta_i \cdot r_A (Y_{AS}, T_S) \tag{2}$$

$$\varepsilon \rho_G c_{pG} \frac{\partial T_G}{\partial t} = \varepsilon \lambda_L \frac{\partial^2 T_G}{\partial z^2} - u \rho_G c_{pG} \frac{\partial T_G}{\partial z} + \alpha a_v \left(T_S - T_G \right) \tag{3}$$

$$\rho_S \left(1-\varepsilon\right) c_{pS} \frac{\partial T_S}{\partial t} = \left(1-\varepsilon\right) \lambda_S \frac{\partial^2 T_S}{\partial z^2} + \left(-\Delta H_{RA}\right) \rho_{cat} \eta_i r_A \left(Y_{AS}, T_S \right) + \alpha a_v \left(T_S - T_G \right) \tag{4}$$

Initial conditions: $t = 0, \;\; 0 \le z \le L, \;\; Y_{AG} = Y_{Ai}\left(z\right);$

$$T_G = T_{Gi}\left(z\right);$$

$$T_S = T_{Si}\left(z\right); \tag{5}$$

Boundary conditions (Danckwerts type):

$$z = 0, t > 0 \qquad u_0 \cdot \left(Y_{A0} - Y_{AG} \right) = -\varepsilon D_L \frac{\partial Y_{AG}}{\partial z} \tag{6}$$

$$\rho_G \cdot u_0 \cdot c_{pG} \left(T_{G0} - T_G \right) = -\varepsilon \lambda_{LS} \frac{\partial T_G}{\partial z} \tag{7}$$

$$\frac{\partial T_S}{\partial z} = 0 \tag{8}$$

$$z = L, t > 0 \qquad \frac{\partial Y_{AG}}{\partial z} = \frac{\partial T_G}{\partial z} = \frac{\partial T_S}{\partial z} = 0 \tag{9}$$

In the above equations: Y_A- molar fraction of hydrocarbon; C_t - molar density of the gas (total molar concentration); T- temperature; r_A- VOC consumption rate; η_i – internal effectiveness factor; u – superficial velocity of the gas; ρ_{cat}, ρ_S, ρ_G – catalyst density, solid density and gas density; k_G, α - mass and heat gas-solid transfer coefficients; a_v – specific interfacial surface area; ε - void fraction of the bed; c_{pG}, c_{ps} – specific heats of gas and solid; D_L, λ_L – effective gas phase transport coefficients by axial dispersion; λ_s – effective thermal conductivity of packed bed; ΔH_{RA}- reaction enthalpy; the indices G and S refer to the gaseous and solid phase values, whereas the index 0 for the values at the inlet of the packed bed.

The duration between two successive flow reversals instants is called semi-cycle or half-cycle (t_{sc}) and its twofold value is called cycle or period ($t_c=2\cdot t_{sc}$). At the initial moment of the first semi-cycle, the packed bed is considered at uniform temperature and zero VOC concentration. The initial conditions of all other semi-cycles were considered identical with the states at the final moment of the preceding ones.

Equations of heat and mass balance (1) to (4) define a system of nonlinear partial differential equations (PDE) which was integrated numerically by finite difference method [7].

For the simulations, it was considered a commercial Pt/γ-alumina catalyst having the Pt distributed in the outer zone of the pellet (0.5 wt % Pt on the average in the pellet). This distribution was approximated by a step function of radial coordinate, with Pt placed in a zone close to the external surface (Figure 2). The Pt concentration in the active zone was so calculated to match an average pellet concentration of 0.5 % by weight.

The chemical reaction considered in the study is the combustion of a hydrocarbon A (in the class of VOC's) having a first order kinetics:

$$r_A = k_0 e^{\left(-\frac{E_A}{RT}\right)} C_A \tag{10}$$

The Pt exploitation efficiency was expressed by the internal effectiveness factor. Due to the low hydrocarbon concentration, its transport inside the porous pellet is characterized by Fick's law with an effective diffusion coefficient incorporating the molecular and Knudsen diffusion.

The reactant concentration dependence on radial position, in the active spherical zone containing Pt, of thickness δ_c, (Figure 2), deduced from mass balance equation of A, is given by equation (11):

$$C_A(\xi) = \frac{C_{AS}}{\xi} \cdot \frac{\xi_1 \varphi \cosh \varphi(\xi - \xi_1) + \sinh \varphi(\xi - \xi_1)}{\xi_1 \varphi \cosh \varphi(1 - \xi_1) + \sinh \varphi(1 - \xi_1)}, \text{ for } \xi_1 \le \xi \le 1 \tag{11}$$

$$\varphi = R\sqrt{\frac{k_v}{D_{ef}}}; \quad \xi = \frac{r}{R}; \quad \xi_1 = \frac{r_1}{R}; \quad k_v = \rho_{cat} k \tag{12}$$

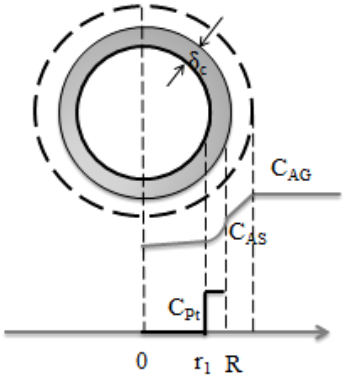

Figure 2. Pt distribution inside the catalyst pellet

Following the usual procedure, one obtains the expression of the effectiveness factor:

$$\eta_i = \frac{\overline{r}_A}{r_A(C_{AS})} = \frac{3}{\left(1-\xi_1^3\right)\varphi^2} \frac{\left(\xi_1\varphi^2 - 1\right)\sinh\varphi\left(1-\xi_1\right) + \varphi\left(1-\xi_1\right)\cosh\varphi\left(1-\xi_1\right)}{\xi_1\varphi\cosh\varphi\left(1-\xi_1\right) + \sinh\varphi\left(1-\xi_1\right)} \tag{13}$$

$\overline{r}_A$ - average reaction rate in the active zone of the pellet;

C_{AS} – VOC concentration at the mouth (entry) of the pores.

The values of physical constants and parameters involved in the mathematical model are given in Table 1.

Considering the limited accuracy of the published correlations for the calculation of gas - solid mass and heat transfer coefficients and for the axial dispersion transport coefficients, these were evaluated by averaging the values calculated from several correlations [3, 8-14].

RESULTS AND DISCUSSION

Influence of internal diffusion

The evolutions of reactant concentration in the spherical catalyst pellet, for various thicknesses of active zone, are shown in Figure 3A (note that ξ_1=0 corresponds to uniform Pt distribution inside the pellet). The less pronounced concentration decrease throughout the pellet corresponds to uniform Pt concentration. When the active zone gets narrower, the decrease of reactant concentration becomes steeper. This result is explained by the

rise of Pt concentration and consequently rise of the combustion rate, combined with the shortening of the diffusion length, with the narrowing the active zone. This feature justifies the superiority of platinum distribution on a narrow area in the immediate vicinity of the external surface.

Table 1. Values of the model parameters

d_R (m)	0.14
L_t(m)	0.6
L_c(m)	0.3
d_p (m)	0.003
ε	0.4
λ_s (J m^{-1} s^{-1} K^{-1})	0.18
ρ_s (kg m^{-3})	1634
c_{ps} (J kg^{-1} K^{-1})	1100
k_0 (s^{-1})	0.18
E_A (J mol^{-1})	82900
ΔH_{RA} (J mol^{-1})	- 802880
p (N m^{-2})	100000
T_0 (K)	293
M (kg $kmol^{-1}$)	29
u_0 (m s^{-1})	0.1
c_{pG} (J kg^{-1} K^{-1})	1015
Y_{A0}	0.001
ΔT_{ad}	27
δ_c (mm)	0.4

The dependence of the internal effectiveness factor on the thickness of the active zone is shown in Figure 3B. The effectiveness factor decreases with the increase of active zone thickness, due to the increase of the diffusion distance (thickness δ_c of the active zone).

Startup and pseudo-steady-state

At the startup of operation, the temperature of the solid bed has to be sufficiently high in order to allow the reaction ignition. In practice, the non-stationary operated reactors are equipped with a solid preheating device, such as gas burners or electric sources [15].

The calculated profiles of hydrocarbon conversion and temperature along the reactor bed at different times during the first two half-cycles are presented in Figure 4. As seen, due to the gas heating, near the feed section appears a colder zone of solid, which is progressively extending in the direction of gas flow (Figures 4 - A2, B2, C2). Note also that the temperatures of the gas and solid are practically equal along the bed. In time, due to the heat generation in the chemical reaction, appears a temperature maximum along the catalyst zone, which is also moving slowly in the gas flow direction.

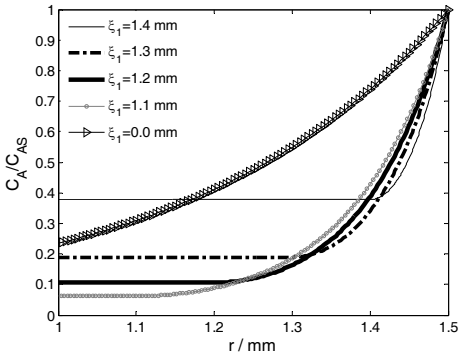

Figure 3A. Reactant concentration profiles in the spherical pellet with different thicknesses of active zone (T=277 °C, R=1.5 mm)

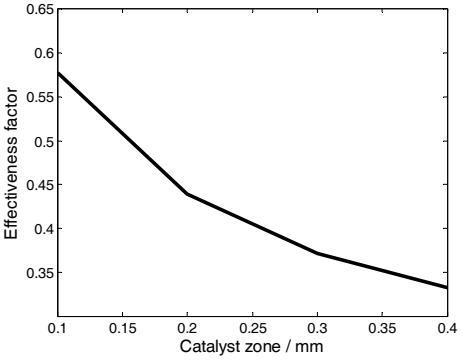

Figure 3B. The internal effectiveness factor versus the thickness of active zone, in the spherical pellet (T=277 °C, R=1.5 mm)

In order to achieve a stable operation, the advancement of cooled zone has to be limited to the entry region of catalyst zone, thereafter the gas flow direction having to be reversed. After the gas flow direction is changed, a new cooled solid zone develops in the new flow direction. In addition, the former cooled zone of the bed is continuously heated, by the gaseous mixture leaving the reaction zone (Figure 4B).

If the half-cycle duration is not excessively high, after a sufficient number of changes of the gas flow direction, it can be achieved the so-called pseudo-steady-state regime. This regime is characterized by identical temperature and conversion profiles along the reactor, when traversed by the gas in the two directions. The computations evidenced that, depending on the operating conditions, the pseudo-steady state regime is practically achieved in the first 50 half-cycles. There are also two observations worth to be added, regarding the conversion profiles in Figure 4: (i) during the semi-cycle interval occurs a small decline of conversion, that can be limited by shortening the semi-cycle duration; (ii) for the duration of the first seconds after the gas flow reversal, appears a temporary zone with higher VOC concentration (smaller conversion values), due to the VOC hold-up retained in the voids of entry zone, in the preceding semi-cycle.

The mechanism of process stabilization can be illustrated through the heat balance terms around the reactor over a time interval, *t*, given by the equation:

$$Q_R(t) + Q_{CS}(t) = Q_P(t) \tag{14}$$

- the amount of heat withdrawn by gas mixture from the bed :

$$Q_P(t) = \int_0^t D_m c_{pG}[T_G(\tau, L) - T_{G0}]d\tau \tag{15}$$

- the amount of heat lost by the solid:

$$Q_{CS}(t) = \int_0^L S\rho_s(1-\varepsilon)c_{ps}[T_s(0,z) - T_s(t,z)]dz \tag{16}$$

- amount of heat released in the combustion reaction:

$$Q_R(t) = \int_0^t D_{MA,0}(-\Delta H_{RA}) \cdot X_A(\tau, L)d\tau \tag{17}$$

Theoretically, the achievement of pseudo-steady state is demanding symmetrical solid temperature profiles along the bed, at the beginning and the end of a semi-cycle:

$$T_{(z)}^{(0)} = T_{(L-z)}^{(t_{sc})} \tag{18}$$

Consequently, the heat (enthalpy) content of the solid should be the same, at the beginning and at the end of a semi-cycle ($Q_{cs}(t_{sc})=0$). The percentage error in fulfilling the heat balance equation, on a pseudo-steady state semi-cycle, has the expression:

$$e = \frac{Q_{CS}(t_{sc}) + Q_R(t_{sc}) - Q_P(t_{sc})}{Q_{CS}(t_{sc}) + Q_R(t_{sc})} 100 \tag{19}$$

Considering a grid of 300 points along the packed bed axis, the calculated percentage error was less than 3% for all simulated semi-cycles, indicating an acceptable accuracy of numerical solution. The improvement of integration accuracy is possible by increasing the number of grid points along the reactor bed.

The diagrams in Figure 5 illustrate the time evolutions for Q_P, Q_R and Q_{CS}, during various semi-cycles, for a duration, t_{sc}=2200 s. The diagram in Figure 5A evidences that the quantity of heat removed from the bed by the gaseous mixture is negligible during a first time interval of the semi-cycle, all the heat generated in reaction being accumulated in the solid bed (Q_{CS} <0). This is explained by existence of a final cold solid zone (ahead of the bed exit), which is cooling the gas down to the feed temperature, while the solid in this zone is gradually heated. After the final zone of the bed is heated above the feeding temperature (T_{G0}), the outlet gas temperature and the heat removed by the gas, start to rise.

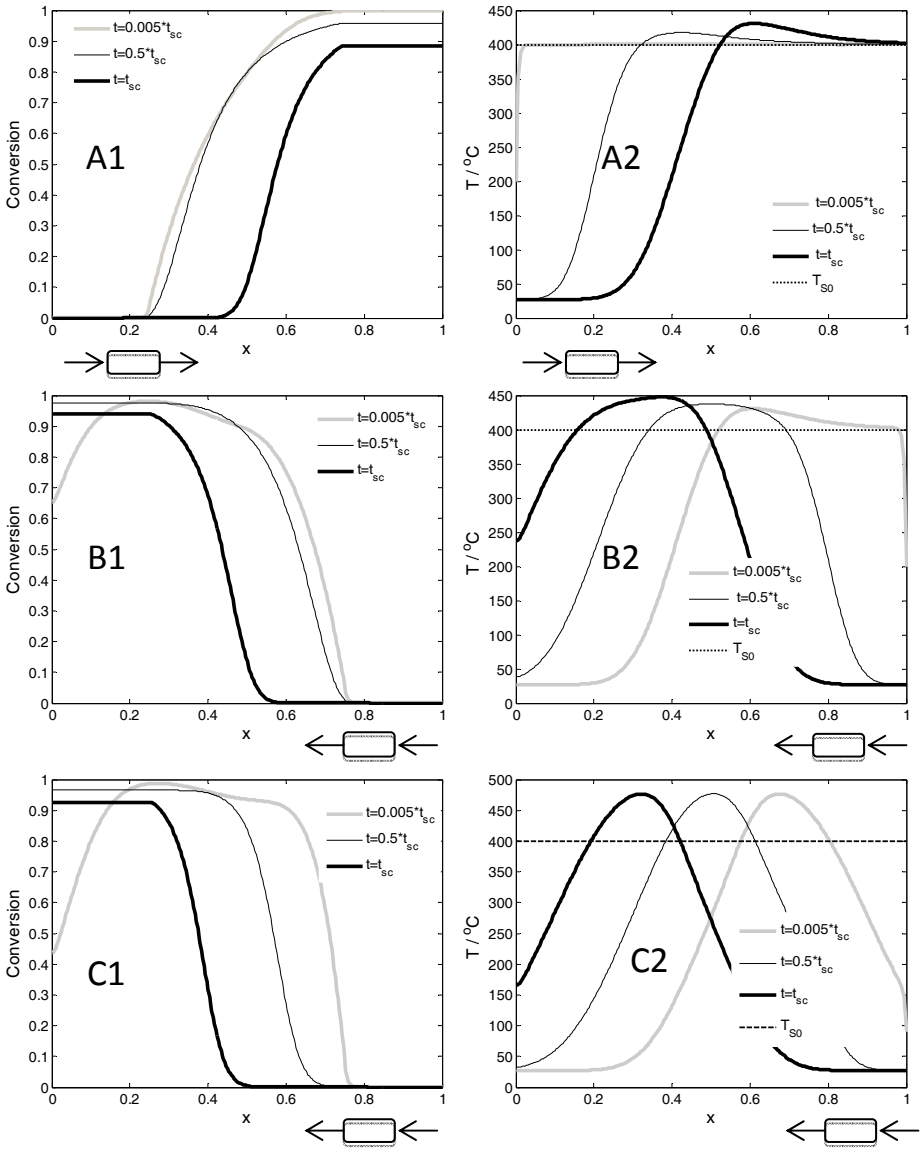

Figure 4. Axial evolutions of conversion and temperature in the reactor at different times during a semi-cycle : A –first semi-cycle; B-second semi-cycle; C – a semi-cycle of stabilized pseudo-steady state (t_{sc}=2200 s, v_0=0.1 m/s, y_0= 0.001, T_{si}=400 °C, L_c=0.3 m, L_t=0.6 m, x=z/L_t)

In the semi-cycles prior to stabilization, the amount of the total heat withdrawn by gas from the bed is greater than the total amount of heat released in the chemical reaction ($Q_P(t_{sc}) > Q_R(t_{sc})$). As seen in diagrams of Figure 5, the stabilization consists in continuously decreasing the total amount of heat removed by the gas stream from the bed during the semi-cycle ($Q_P(t_{sc})$) until it equals the total amount of heat released in chemical reaction ($Q_R(t_{sc})$). At this point, the total heat lost from the solid becomes zero during a half cycle ($Q_{CS}(t_{sc}) = 0$), which means the same heat content of solid bed at the beginning of each half cycle (Figure 5B). The diagram in Figure 5C shows an approximately linear increase of total heat released in reaction with the time, due to the fact that the rate of heat generation is approximately constant (almost constant conversion of hydrocarbon during the semi-cycle).

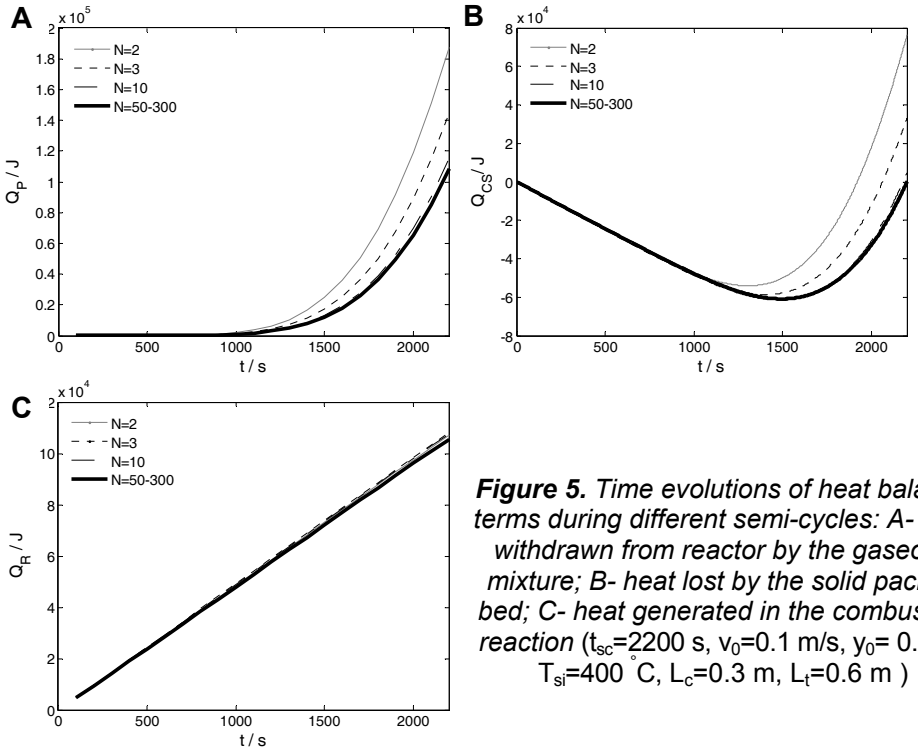

Figure 5. *Time evolutions of heat balance terms during different semi-cycles: A- heat withdrawn from reactor by the gaseous mixture; B- heat lost by the solid packed bed; C- heat generated in the combustion reaction* (t_{sc}=2200 s, v_0=0.1 m/s, y_0= 0.001, T_{si}=400 °C, L_c=0.3 m, L_t=0.6 m)

From the analysis presented above, it follows that the pseudo-steady state is achieved if total amount of heat removed by the gas from the bed during a half cycle equals the amount of heat released in the reaction during the same duration, $Q_P(t_{sc}) = Q_R(t_{sc})$.

If the total heat released in the reaction over a half cycle is smaller than the total heat removed by the gas ($Q_P(t_{sc}) > Q_R(t_{sc})$), the heat content of the bed and consequently its average temperature, gradually decrease, leading to reaction extinction.

These results show that the stable auto-thermal operation of the reverse flow reactor is achieved by continuously changing the solid temperature profile along the bed, keeping adequate levels and width to accomplish the chemical transformation. This occurs by successive heat accumulation and heat removal steps, leading to identical heat content of the bed at the beginning and the end of a semi-cycle.

During a stabilized semi-cycle, it is transferred a quantity of heat from the first zone of the bed contacted by gas, towards the final bed region, the gas acting as a heat carrier. On overall, as already emphasized, the amount of heat generated in reaction during a semi-cycle is entirely withdrawn from the bed by the gas. This is a feature worth to underline, some authors asserting that the principle of RFR operation consists simply in the accumulation of combustion heat into the bed.

An inconvenient of reverse flow reactor consists in small non-reacted VOC emissions occurring at changes in gas flow direction (Figure 6). At the end of each semi-cycle, throughout the cooled feed zone of solid is accumulated an amount of hydrocarbon, which is pushed out immediately after the change of the gas flow direction. The duration of this emission is very short, having the order of magnitude equal to the gas residence time into the cooled zone of the bed. In the simulated conditions, after approximately 1.5 seconds from the change of flow direction, there are no significant amounts of hydrocarbon eliminated from the reactor (Figure 6B), these being stabilized to a level dependent on VOC conversion achieved in the bed. Note that the top points in the diagram shown in Figure 6C represent the concentration of hydrocarbon at the exit of the bed, when changing the direction of gas flow. To minimize the unreacted VOC emissions, the duration of the semi-period should be kept close to its maximum possible value. However, the increase of semi-cycle duration could induce some decrease of hydrocarbon conversion, due to the extension of the cooled zone of the bed.

Influence of operating parameters

(i) Influence of main operating parameters on the maximum semi-cycle duration

As already mentioned, for a given set of operating parameters, the pseudo-steady state can be achieved for any duration of semi-cycle, inferior to a limit called maximum duration of semi-cycle. The simulation results presented in Figure 7 shows stabilized temperature evolutions along the packed bed (obtained

after 300 periods) in different working conditions and the corresponding maximum semi-period duration. These are evidencing that the maximum semi-period duration is increased by decreasing the gas velocity, increasing the feed hydrocarbon concentration, increasing the initial temperature of the packed bed and (in some limits) by increasing the catalyst to inert amounts ratio.

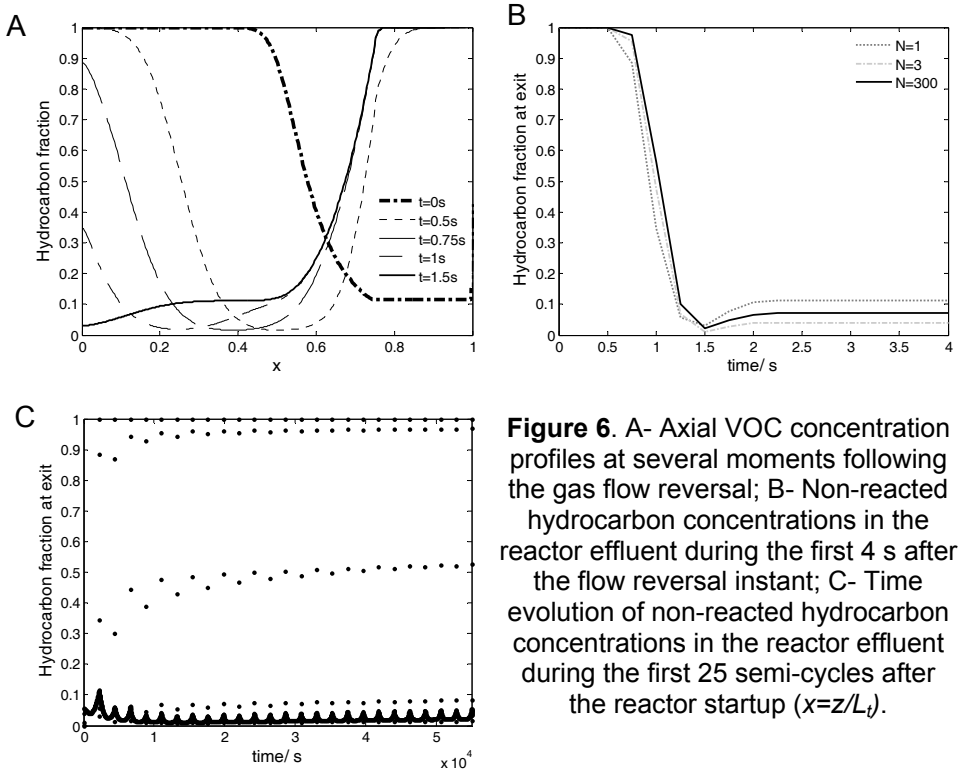

Figure 6. A- Axial VOC concentration profiles at several moments following the gas flow reversal; B- Non-reacted hydrocarbon concentrations in the reactor effluent during the first 4 s after the flow reversal instant; C- Time evolution of non-reacted hydrocarbon concentrations in the reactor effluent during the first 25 semi-cycles after the reactor startup ($x=z/L_t$).

The following general conclusions can be drawn from Figures 7 A, B, C and D: (i) By increasing the gas velocity (or equivalently the flow rate) the cooling capacity of the gas is raised and the velocity of cooled zone extension increases, narrowing the hot zone of the bed. (ii) Increasing the feed hydrocarbon concentration, it is also increased the amount of reactant consumed and consequently the amount of heat generated inside the bed, leading to the raise of maximum solid temperature. As known, the increase of temperature in a catalyst bed has to be controlled, as it may be harmful for the catalyst activity. A similar effect has also the increase of startup temperature of the solid. (iii) Extending the catalyst zone width in detriment of the inert zone, can also increase, in some limits, the maximum duration of

semi-cycle. Nevertheless, the cooling effect prevails, so that the duration of the half-cycle is subject to the phenomenon of overlapping the high-temperature front with catalytically active zone, which assure the occurrence of chemical reaction with adequate intensity.

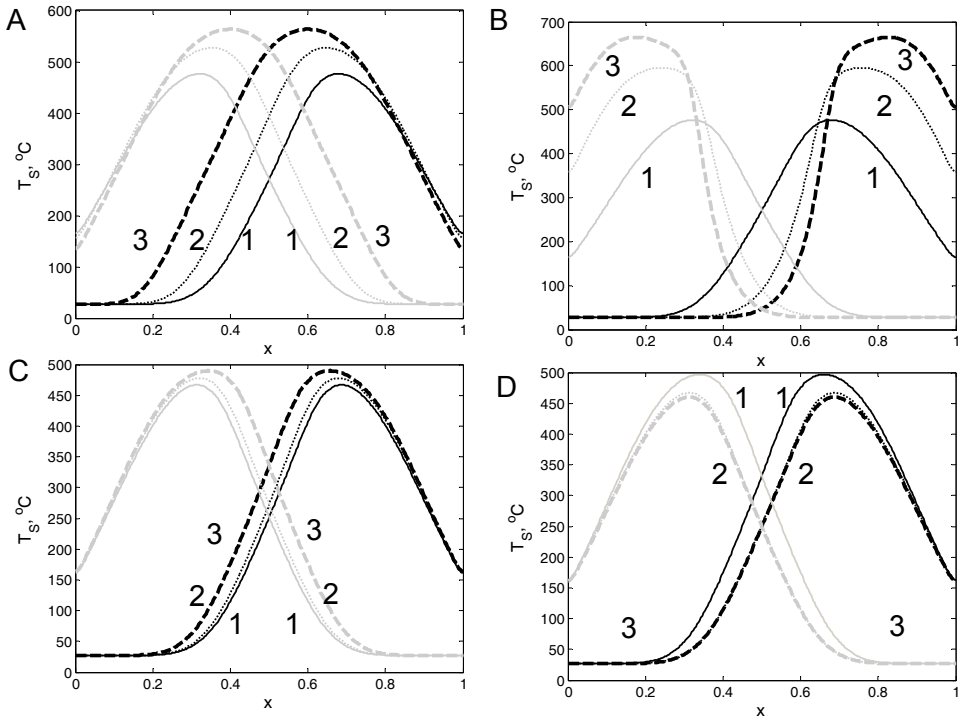

Figure 7. Stabilized axial temperature evolutions (achieved after 300 periods) and maximum semi-cycle durations in different working conditions (grey curves - direct feed, black curves - reverse feed, $x=z/L_t$). Nominal values: T_{si}= 400 °C, y_0= 0.001, v=0.1 m/s, L_t=0.6 m, L_c=0.3 m. A (1- v=0.1 m/s, t_{sc}=2200 s; 2 - v=0.2 m/s, t_{sc}=900 s; 3- v=0.3 m/s, t_{sc}=400 s); B (1- y_0=0.001, t_{sc}=2200 s; 2 - y_0=0.002, t_{sc}=3300 s; 3- y_0=0.003, t_{sc}=3800 s;); C (1- T_{si}=400 °C, t_{sc}=2250 s; 2- T_{si}=375 °C, t_{sc}=2200 s; 3- T_{si}=350 °C, t_{sc}=2000 s); D (1- L_c=0.24 m, t_{sc}=2000 s; 2 - L_c=0.30 m, t_{sc}=2250 s; 3- L_c=0.42 m, t_{sc}=2250 s)

(ii) Influence of operating parameters on process evolution at given semi-period duration

The curves in Figure 8A show the influence of gas flow rate on the final axial temperature profile, corresponding to a semi-period duration of 400 s. As the gas flow rate increases, the hot zone width decreases and the combustion reaction releases a significant quantity of heat in a narrower catalyst bed, leading to more significant peak temperature. As underlined

above, the maximum semi-period get lower with the increase of gas flow rate, so that it is preferred to operate at lower gas flow rates, in order to guarantee high conversions for higher maximum semi-period duration. The diagram in Figure 8B illustrates the influence of feed concentration on final temperature profiles along the bed. As expected, the width of hot zone and the maximum temperature augment with the rise of feed hydrocarbon concentration, as result of increasing the amount of heat generated in the bed.

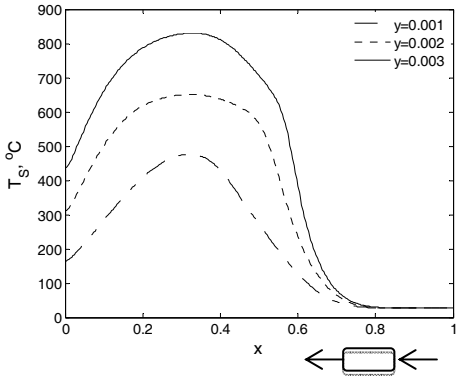

Figure 8B. Stable final temperature profiles along the bed at different feed concentrations and constant semi-period duration (t_{sc}=2200 s).

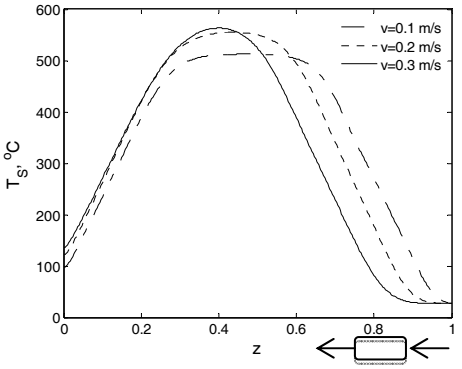

Figure 8A. Stable final temperature profiles along the bed at different gas flow rates and constant semi-period duration (t_{sc}=400 s)

As already underlined, unexpected increases of feed concentration present the danger of excessive temperatures in the bed, whereas the decrease of feed concentrations is inducing a decrease in hydrocarbon conversion, diminishing the heat released in the chemical reaction, with potential danger to light-off the chemical reaction. These effects can be compensated by changing (increasing or decreasing) the gas flow rate passing through the reactor.

Simulation calculations evidenced also that, for a given semi-period, the initial temperature of the solid bed (if adequate) does not influence the final temperature profile, it playing a role only in the process evolution toward the pseudo-steady state regime.

CONCLUSIONS

The operation of packed bed catalytic reactors with periodical change of flow direction is a technique that permits auto-thermal operation, even for very low feed concentration of reactant, a feature that makes it very attractive for gas cleaning by catalytic combustion. The stabilization of transient operation

is possible when the heat removed by the gas from the bed during a semi-cycle, equals the amount of heat generated in combustion reaction. For given values of working parameters, there exists a maximum semi-cycle duration, below which is possible the process stabilization. The simulation results of this work evidence the influences of the main process parameters on the process dynamics and on the maximum semi-cycle duration.

REFERENCES

1. Y.S. Matros, G.A. Bunimovich, *Catalysis Rev.-Sci. Eng.*, **1996**, *38*, 1;
2. Y.S. Matros, "Catalytic Processes under Unsteady-State Conditions", Elsevier, **1989**, chapter 3;
3. B. van de Beld, "Air Purification by Catalytic Oxidation in an Adiabatic Packed Bed Reactor with Periodical Flow Reversal", PhD thesis, Twente University, The Netherlands, **1995**;
4. A.A. Barresi, M. Vanni, M. Brinkmann, G. Baldi, *AIChE Journal*, **1999**, *45*, 1597;
5. A.A. Barresi, I. Mazzarino, Vanni M., G. Baldi, *The Chemical Engineering Journal*, **1993**, *52*, 79-88;
6. G. Kolios, J. Frauhammer, G. Eigenberger, *Chemical Engineering Science*, **2000**, *55*, 5945;
7. A.V. Wouwer, P. Saucez, W.E. Schiesser, "Adaptive method of lines", Chapman & Hall/CRC Press, **2001**, chapter 1;
8. K.R. Westerterp, W.C. Kusters, R.J. Wijngaarden, *Chem. Ing. Tech*, **1984**, *56*, 621;
9. G. Bozga, O. Muntean, „Reactoare Chimice", Ed. Tehnică, Bucharest, **2001**, chapter 5;
10. N. Wakao, S. Kaguei, „Heat and Mass Transfer in Packed Beds", Gordon and Breach Science Publishers, Inc., New York, **1982**, chapter 4, 5;
11. S. Salomons, R.E. Hayes, M. Poirier, H. Sapoundjiev, *Computer and Chemical Engineering*, **2004**, *28*, 1599;
12. B. Koning, "*Heat and Mass Transport in Tubular Packed Bed Reactors at Reacting and Non-Reacting Conditions"*, PhD thesis, Twente University, The Netherlands, **2002**;
13. R.E. Hayes, „Introduction to catalytic combustion", Gordon and Breach Science Publishers, Inc., Canada, **1997**, chapter 3;
14. J. Smit, M. van Sint Annaland, J.A.M. Kuipers, *Chemical Engineering Science,* **2005**, *60*, 6971;
15. M. Brinkmann, A.A. Barresi, M. Vanni, G. Baldi, *Catalysis Today*, **1999**, *47*, 263.